IJC
International Journal of Cancer

Targeting of the P2X7 receptor in pancreatic cancer and stellate cells

Andrea Giannuzzo[1]*, Mara Saccomano[2]*, Joanna Napp[2,3,4], Maria Ellegaard[5], Frauke Alves[2,3,4] and Ivana Novak[1]

[1] Section for Cell Biology and Physiology, August Krogh Building, Department of Biology, University of Copenhagen, Denmark
[2] Department of Molecular Biology of Neuronal Signals, Max Planck Institute for Experimental Medicine, Hermann-Rein-Straße 3, Göttingen, D-37075, Germany
[3] Department of Haematology and Medical Oncology, University Medical Center Göttingen, Robert-Koch-Str. 40, Göttingen D-37075, Germany
[4] Department of Diagnostic and Interventional Radiology, University Medical Center Göttingen, Robert-Koch-Str. 40, Göttingen D-37075, Germany
[5] Departments of Clinical Biochemistry and Endocrinology, Rigshospitalet, Research Center for Ageing and Osteoporosis, Glostrup, Denmark

The ATP-gated receptor P2X7 (P2X7R) is involved in regulation of cell survival and has been of interest in cancer field. Pancreatic ductal adenocarcinoma (PDAC) is a deadly cancer and new markers and therapeutic targets are needed. PDAC is characterized by a complex tumour microenvironment, which includes cancer and pancreatic stellate cells (PSCs), and potentially high nucleotide/side turnover. Our aim was to determine P2X7R expression and function in human pancreatic cancer cells *in vitro* as well as to perform *in vivo* efficacy study applying P2X7R inhibitor in an orthotopic xenograft mouse model of PDAC. In the *in vitro* studies we show that human PDAC cells with luciferase gene (PancTu-1 Luc cells) express high levels of P2X7R protein. Allosteric P2X7R antagonist AZ10606120 inhibited cell proliferation in basal conditions, indicating that P2X7R was tonically active. Extracellular ATP and BzATP, to which the P2X7R is more sensitive, further affected cell survival and confirmed complex functionality of P2X7R. PancTu-1 Luc migration and invasion was reduced by AZ10606120, and it was stimulated by PSCs, but not by PSCs from P2X7$^{-/-}$ animals. PancTu-1 Luc cells were orthotopically transplanted into nude mice and tumour growth was followed noninvasively by bioluminescence imaging. AZ10606120-treated mice showed reduced bioluminescence compared to saline-treated mice. Immunohistochemical analysis confirmed P2X7R expression in cancer and PSC cells, and in metaplastic/neoplastic acinar and duct structures. PSCs number/activity and collagen deposition was reduced in AZ10606120-treated tumours.

Introduction

Pancreatic ductal adenocarcinoma (PDAC) is the most common form of pancreatic cancer, and with a 5-year survival rate <5% it ranks as one of the most deadly cancers.[1,2] This extremely poor prognosis is largely attributed to its propensity for early local invasion and distant metastases and to the asymptomatic development of the early stage of the pancreatic cancer.[3] Consequently, this type of cancer is often not detected until it has already disseminated to surrounding or distant organs and vessels, and therefore most of the current therapies

Key words: P2X7, PDAC, fibrosis, AZ10606120, stellate cells

Abbreviations: α-SMA: alpha-smooth muscle actin; AEC: 3-amino-9-ethylcarbazole; ANOVA: analysis of variance; ATP: adenosine-5′-triphosphate; BLI: bioluminescence imaging; BrdU: bromodeoxyuridine; BzATP: 2'(3')-O-(4-Benzoylbenzoyl) adenosine-5'-triphosphate; DAPI: 4′: 6-diamidino-2phenylindole; DTT: dithiothreitol; ECM: extracellular matrix; EDTA: ethylenediaminetetaacetic acid; EGFR: epidermal growth factor receptor; EMT: epithelial to mesenchymal transition; FBS: fetal bovine serum; GBSS: Gey's balanced salt solution; mPSC: murine pancreatic stellate cells; P2X7R: P2X7 receptor; PanIN: pancreatic intraepithelial neoplasia; PBS: phosphate buffered saline; PDAC: pancreatic ductal adenocarcinoma; PSC: pancreatic stellate cell; PVDF: polyvinylidene difluoride; ROI: region of interest; RT-PCR: reverse transcriptase polymerase chain reaction; SEM: standard error of the mean; siRNA: short interfering RNA; SNP: single nucleotide polymorphism; TBS: tris-buffered saline; TME: tumour microenvironment; TRIS: 2-amino-2-hydroxymethyl-propane-1,3-diol

Additional Supporting Information may be found in the online version of this article.

*A.G. and M.S. contributed equally to this work

Grant sponsor: The European Commission, FP7 Marie Curie Initial Training Network IonTraC; **Grant number:** FP7-PEOPLE-2011-INT 289648; **Grant sponsor:** The Danish Council for Independent Research | Natural Sciences; **Grant number:** DFF 4002-00162; **Grant sponsor:** The Carlsberg Foundation; **Grant number:** 2013-01-0312

DOI: 10.1002/ijc.30380

History: Received 11 Feb 2016; Accepted 1 Aug 2016; Online 11 Aug 2016

Correspondence to: Ivana Novak, Department of Biology, Section for Cell Biology and Physiology, August Krogh Building, Universitetsparken 13, University of Copenhagen, Copenhagen DK-2100, Denmark, Tel.: +45 353-30275, E-mail: inovak@bio.ku.dk

What's new?
Pancreatic ductal adenocarcinoma (PDAC) is one the most difficult types of cancer to detect and treat, challenges that could be overcome through the discovery and development of novel markers and therapeutic strategies. Here, the P2X7 receptor, which regulates cell survival, is shown to also support cell proliferation, migration and invasion in human P2X7R-expressing PDAC cells. Treatment of orthotopic PDAC tumor-bearing mice with the P2X7R-specific inhibitor, AZ10606120, resulted in decreased tumor bioluminescence and reductions in pancreatic stellate cells and collagen deposition. Targeting of P2X7R warrants further investigation as a promising therapeutic approach in pancreatic cancer.

are more palliative then curative. New treatment strategies are therefore desperately needed.[4] There are two main theories about how epithelial cells might drive the tumour development. In the classical model it has been proposed that pancreatic ducts undergo a series of pancreatic intraepithelial neoplasias (PanINs), epithelial to mesenchymal transition (EMT) and progression to invasive cancer.[5] A number of studies support a different model, which proposes that acinar-to-duct metaplasia can give rise to tubular complexes that may occur in parallel and/or progress to PDAC.[6,7] An important cellular component in PDAC are pancreatic stellate cells (PSCs) that secrete extracellular matrix (ECM) proteins, such as collagens and laminin, and contribute to the stiffness and impermeability of these solid tumours, and thus reduced delivery of chemotherapeutic drugs. A number of studies document that coexistence of cancer cells and activated PSCs supports tumour growth and malignancy both *in vitro* and *in vivo* models.[8]

One of the general characteristics of cancer cells is a high metabolic rate and therefore there is a high turnover of intracellular nucleotides/sides. Recently, novel *in vivo* ATP imaging probes revealed relative high levels of extracellular ATP at tumour sites,[9] released to the extracellular compartment by metabolically active cancer cells and dying cells in the tumour necrotic core. Therefore, ATP-activated receptors, *i.e.,* the purinergic receptors (P2X and P2Y), could be important receptors regulating both cancer and stromal cell proliferation, apoptosis and migration.[10]

One of the cancer-relevant receptors is the P2X7 receptor (P2X7R). The receptor exists in several splice isoforms (A–J) and single nucleotide polymorphisms (SNPs) correlate with several diseases.[11,12] The P2X7R is a ligand-gated ion channel permeable to Ca^{2+}, K^+ and Na^+.[13] Following sustained activation or overstimulation, this receptor forms or facilitates formation of pores permeable to large molecules that can lead to cell lysis and death.[14,15] In the cancer field, P2X7R is believed to play multiple roles. First, it can be an anti-tumour receptor inducing cancer cell death.[16,17] Second, P2X7R can also be a procancer receptor, as it supports cancer cell proliferation, migration and invasion, both *in vitro*[18,19] and *in vivo*.[20] One explanation is that these seemingly opposite effects depend on expression/interaction of presumed proapoptotic P2X7A isoform and trophic isoform P2X7B.[21] Third, P2X7R is involved in inflammation and immune system modulation, which can potentially affect tumour growth and progression.[1,22]

Many cancers, such as human breast cancer[18] and human prostate carcinoma,[23] show increased expression of P2X7R. In our recent study, we showed higher expression of P2X7R in several PDAC cell lines compared to noncancer cells and characterized the *in vitro* effect on proliferation and migration/invasion.[24] Also, pancreatic stellate cells express P2X7R and in *in vitro* conditions inhibition of this receptor decreased cell proliferation.[25]

The aim of this study was to determine the role of P2X7R in the *in vivo* model of an orthotopic xenograft human pancreatic cancer. In particular, we wanted to test the effect of the P2X7R allosteric inhibitor AZ10606120. For this purpose we have utilized PancTu-1 cell line expressing the luciferase gene (PancTu-1 Luc) for bioluminescence imaging to follow tumour development and progression in response to P2X7R antagonism. Prior to the *in vivo* study, we validated our approach in *in vitro* assays of PancTu-1 Luc cells by determining P2X7R expression, drugs sensitivity and interplay with PSCs. Here, we show that AZ10606120 has a potential to influence pancreatic tumour growth and limits fibrosis.

Material and Methods

Cell culture

PancTu-1 cells (established by Dr. M. v. Bulow, Mainz, Germany), modified to stably express luciferase (PancTu-1 Luc cells), were kindly donated by Prof. Dr. Holger Kalthoff (University Hospital Schleswig-Holstein, Kiel, Germany). Cells were grown in RPMI-1640 media supplemented with 10% fetal bovine serum (FBS) (PAA Laboratories; A15-151 Gold). For the *in vitro* experiments performed in Copenhagen, 100 U/ml penicillin and 100 μg/ml streptomycin were added to the medium. For the *in vivo* experiments performed in Göttingen, cells were grown without antibiotics. The human pancreatic duct epithelial cell line HPDE6-E6E7 (H6c7) transformed with HPV16,[26] here abbreviated HPDE, was grown as described earlier.[24]

RNA isolation, RT-PCR and western blot

RNA isolation, RT-PCR and Western blot were performed as previously described.[24] The primers used to detect human *P2X7* mRNA were: forward primer: 5′–CGGTTGTGTCCCG AGTATCC–3′ and reverse primer: 5′–CCTGGCAGGATG TTTCTCGT–3′ (284 bp). We performed RT-PCR rather than Real Time-PCR (qPCR), because it is not possible to

design qPCR primers specific for other than the isoform A. For the Western blot, membranes were incubated with primary antibody against P2X7R C-terminal (1:500 rabbit polyclonal, Alomone, APR-004).

SiRNA transfection

PancTu-1 Luc cells were transfected with 50 nM siRNA against P2X7 mRNA (siP2X7) or siRNA Naito-1 (scramble) as control (Tebu-Bio, Roskilde, Denmark), using Lipofectamine RNAiMAX (Invitrogen). Experiments were performed 48 hr after transfection.

Cell proliferation and migration

Cell proliferation and wound assays were performed according to the procedures described earlier.[24] Aphidicolin (5 μM) was used to stop proliferation.

Mouse pancreatic stellate cells (mPSCs) isolation

Animals were handled according to the guidelines by the Danish Animal Experimentation Inspectorate (license no. 2011/561-56). Male Balb/cJ P2X7 wild type mice (Taconic) and Balb/cJ P2X7$^{-/-}$ mice[27] were used for PSC isolation as described earlier[25] with the following modifications: excised pancreas was washed in cold Gey's Balanced Salt Solution (GBSS), suspended in 3 ml of cold GBSS containing 3 mg of Collagenase P (Roche) and cut into small pieces. The suspension was incubated at 37°C for 30 min, then dispersed by pipetting and centrifuged at 1040 g for 8 min at room temperature. The supernatant was removed and the pellet was re-suspended in warm culture media (DMEM/F12 1:1, 10% FBS, 100 U/ml penicillin, 100 μg/ml streptomycin) and transferred to a Petri dish precoated with pure FBS. After 2 hr of incubation at 37°C in 5% CO_2, the media was removed and the dish was washed several times. PSCs remained attached to the bottom of the dish.

Co-culture of mPSCs and PancTu-1 Luc cells

Wild type or P2X7$^{-/-}$ mPSCs (30.000; passage 1–3) were plated in a 24-well plates. After 24 hr PancTu-1 Luc cells (50.000) were plated in the upper chamber of the insert (transparent PET membrane, 8.0 μm pore size, Falcon) with 5 μM Aphidicolin and either with or without AZ10606120 (10 μM). After 48 hr, cells were fixed in cold methanol and stained with Crystal Violet. Bright field images were taken with 10x objective in Leica DMI6000B microscope. Cells were counted using ImageJ (version 1.47, National Institute of Health, Bethesda, MD).

Orthotopic PancTu-1 Luc pancreatic tumour mouse model

This study was approved by the administration of Lower Saxony (Germany) and animals were handled according to the guidelines issued by the animal protection (licence no. 33.9–42502-04–13/1085). Experiments were performed on 10–19 weeks old male athymic nude mice (NMRI-*Foxn1*^{nu}) bred in the Animal Facility of the University Medical Center Göttingen. Animals were housed in individual-ventilated cages (IVS) and allowed food and water ad libitum. For orthotopic transplantation, mice were anesthetized by intraperitoneal (i.p.) injection of 15 mg/kg xylazine and 75 mg/kg ketamine. PancTu-1 Luc cells grown in media without antibiotics were harvested with 0.25% trypsin-EDTA solution and washed twice with medium. The 1×10^6 cells were re-suspended in 20 μl of sterile PBS and injected in the head of the pancreas (Fig. 1*a*) as previously described.[28] Mice were weighed and inspected twice a week for weight loss, general condition and tumour formation.

Treatment schedule

Animals were randomly divided into two groups treated with either 5 mg/kg AZ10606120 re-suspended in NaCl 0.9% (1 mg/ml) ($n = 7$) or with NaCl 0.9% ($n = 6$) alone as vehicle control (i.p. injection was performed every other day for both treated and control groups). Treatment started 10 days after implantation of cancer cells, and was continued every second day until sacrifice on Day 30 (Fig. 1*b*).

Bioluminescence imaging

In order to assess primary tumour growth *in vivo* over time in response to therapy, Bioluminescence imaging (BLI) measurements were done at Day 10, 17, 23 and 30, and treatments were started after the first measurement at day 10. Mice were injected i.p. with 50 mg/ml of D-luciferin (Promega) dissolved in sterile PBS at a dose of 150 mg/kg body weight. Ten minutes after D-luciferin injection, mice were placed on the stage of the IVIS-Spectrum (PerkinElmer) and imaged with CCD using default bioluminescence settings of Living Image 4.4 software (open filter configuration, automatic exposure time, F/Stop = 1) with medium binning. A sequence of five images (segments) with a delay of 1 min each was acquired. To quantify the *in vivo* signal intensity over time, regions of interest (ROIs) encompassing the entire primary tumour mass were placed on the 2D bioluminescence images acquired 15 min (maximum intensity) after D-luciferin injection and total flux (photon/sec) over this area were calculated.

At Day 30, mice were scanned again *in vivo* and then sacrificed and scanned *ex vivo* with opened abdominal cavity by IVIS Spectrum using the same parameters mentioned above. Immediately afterwards, the tumour together with the stomach and duodenum was removed and also scanned with BLI. Tumour sizes were measured with caliper and volumes were calculated using the formula: volume [mm^3] = 0.5 × (length × width × height). Grade of invasion into stomach and duodenum was macroscopically evaluated and the occurrence of ascites and jaundice, grade of tumour invasion in the surroundings organs and size, numbers and location of metastases were recorded. Subsequently, *ex vivo* bioluminescence imaging was performed on excised organs such as spleen, liver, kidney, intestine and mesenteries to confirm the presence of metastases.

Immunohistochemistry and analysis of the stained tissues

Organs were placed in 10% buffered formalin and embedded in paraffin for further histological evaluation. Slices (2 μm

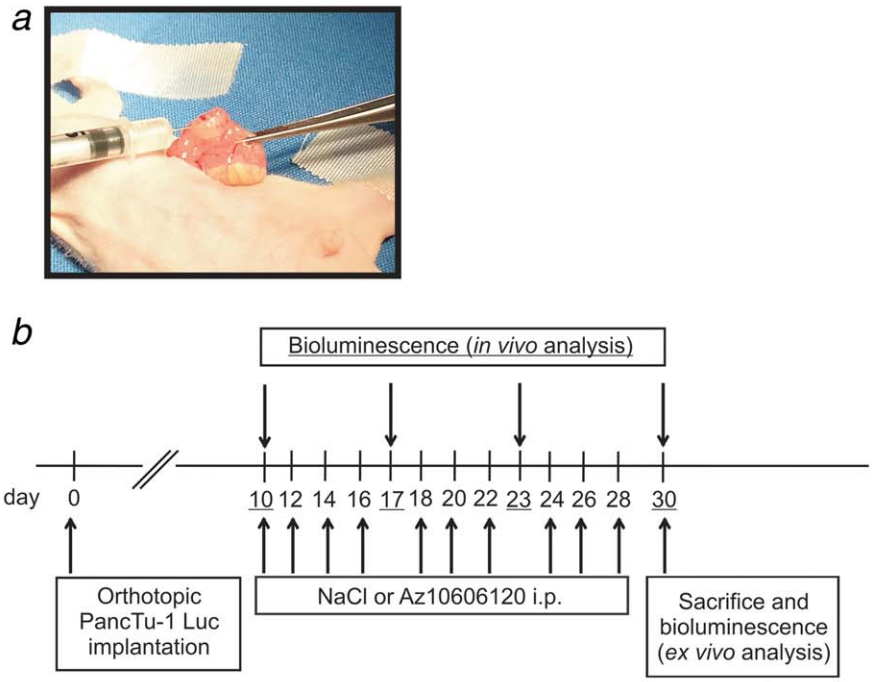

Figure 1. Orthotopic implantation of PancTu-1 Luc cells and timeline of AZ10606120 therapy. (*a*) PancTu-1 Luc cells injection in the head of pancreas of a nude mouse at day 0. (*b*) Schematic diagram of the experimental protocol used for the treatment with AZ10606120 and for the bioluminescence analysis. [Color figure can be viewed in the online issue, which is available at wileyonlinelibrary.com.]

thick) were deparaffinized and rehydrated according to standard procedures, and pretreated at 98°C for 20 min in citrate buffer (pH 6.0, Dako). Slides were incubated for 10 min with 3% H_2O_2 or 0.1 M TRIS-glycine (pH 7.4) for chromogenic and fluorescent detection, respectively. Afterward, slides were incubated with Protein Block (Dako) or Blocking Buffer–Fish (SurModics) for 20 min to block unspecific protein binding. Slides were incubated with the rabbit polyclonal antibody anti-P2X7 C-terminus (Alomone APR-004, 1:200), or one of the two rabbit anti-P2X7 extracellular loop antibodies (Alomone APR-008, 1:200 or Life Technologies PA5-28020, 1:900), or the monoclonal rabbit anti-human EGFR (Life Technologies MA5-16359, 1:100), or the polyclonal rabbit anti-alpha smooth muscle actin (Abcam AB5694, 1:500). Overnight incubation at 4°C was followed by treatment with N-Histofine Simple Stain Max PO anti-rabbit (Nichirei) for 1 hr and staining with 3-Amino-9-ethylcarbazole (AEC). All slides were counterstained with Mayer hematoxylin (Merck). For the fluorescence detection, the slides were incubated with the relevant secondary antibody conjugated to Alexa Fluor-568 or Alexa Fluor-488 (Life Technologies, 1:400) for 1 hr, or directly incubated with the polyclonal antibody rabbit anti-P2X7 receptor (extracellular)-ATTO-488 (Alomone APR-008-AG, 1:400) overnight at 4°C. DAPI (Molecular Probes) was used for nuclear staining.

The collagen I/III and the connective tissue we detected with the Picrosirius Red Stain Kit (24901, Polysciences) and the Masson Goldner Trichrom Kit (12043, Morphisto), respectively. After deparaffinization and rehydration, tissue sections were stained with Weigert hematoxylin (Morphisto) according to the manufacturer's instructions. Bright field and immunofluorescence pictures were taken in Leica DMI6000B microscope and Leica SP 5X MP confocal laser scanning microscope, respectively. Image J software was used to analyse the images. To quantify PSCs and collagen, slides were stained for α-SMA and Picrosirius Red. Images (8–9 fields of view per slide in each animal) were thresholded, converted into binary images and the stained area was calculated.

Chemicals and statistics

All chemicals/kits were purchased from Sigma-Aldrich unless otherwise stated. Data are shown as mean values ± standard error of mean (SEM) and n represents the number of biological replicates. Statistical analysis on data was performed by using Students t test and one-way analysis of variance (ANOVA) with Bonferroni method using SigmaPlot 11.0. Data were analyzed in Origin or Microsoft Excel.

Results

PancTu-1 Luc cells express P2X7R

In order to use the human PancTu-1 Luc pancreatic cancer cells in the orthotopic xenograft mouse model, we first determined whether cells express P2X7R and investigated their behavior in an *in vitro* setting, similar to our studies on other PDAC cells.[24] HPDE cells were used as control. Transcripts for *P2X7* in HPDE and PancTu-1 Luc cells were detected by

RT-PCR (Fig. 2*a*). Western blot analysis using an antibody against P2X7R C-terminus (Fig. 2*b*) shows that both cell lines express the full length P2X7R isoform (70 kDa). Notably, PancTu-1 Luc cells showed a higher protein level compared to the HPDE control cells.

Role of P2X7R in cell proliferation

Effect of ATP stimulation on proliferation of PancTu-1 Luc cells was determined using BrdU assay (Fig. 2*c*; black bars). There was a significant reduction of about 20% in BrdU incorporation already with 10 μM ATP compared to the control (no exogenous ATP). With 100 μM ATP this reduction became more pronounced (about 80%), and it remained similar with 1 mM ATP. The treatment with allosteric P2X7R inhibitor AZ10606120 (10 μM; Fig. 2*c*, white bars) reduced BrdU incorporation (80%) at both basal conditions and at low ATP concentrations (0 or 10 μM). This effect was most likely due to an arrest of proliferation, since AZ10606120 is not cytotoxic at 10 μM concentration.[29] Moreover, the inhibitor in combination with higher ATP concentrations (100 μM to 1 mM) further reduced BrdU incorporation, due to a stop of proliferation caused by the inhibitor and potentially due to cell death induced by high ATP concentrations, similar to effects detected on other PDAC cells.[24] We also used BzATP, which is often used to stimulate P2X7R, though some reports claim activation of other P2 receptors.[24,30] The reduction in BrdU incorporation became apparent at 100 μM and 1 mM of BzATP, (Fig. 2*d*). In order to confirm that P2X7R is involved in cell survival, we performed studies where the receptor was silenced using siRNA. Results in Figures 2*e*–2*f* show that knockdown of the receptor caused decreased BrdU incorporation indicating reduced proliferation. Addition of BzATP (100 μM), which would have reduced BrdU incorporation in control conditions, lost its effect in cells treated with siRNA.

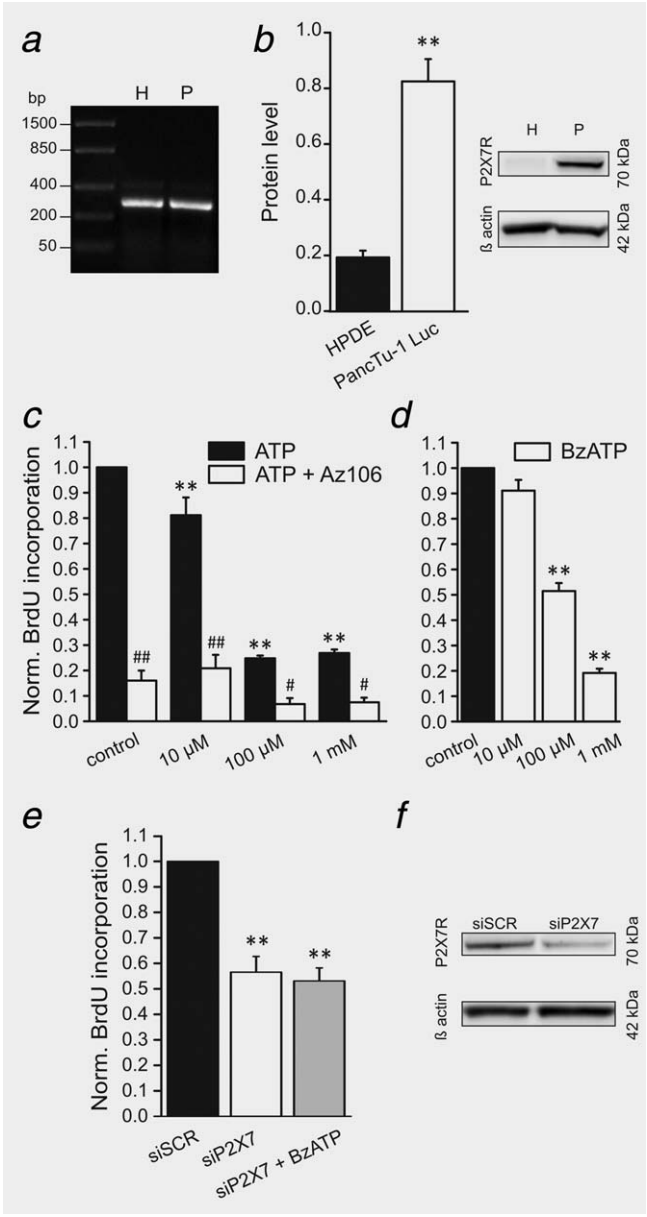

Figure 2. Expression of P2X7R and cell proliferation with ATP, AZ10606120 and BzATP. (*a*) Representative gel of *P2X7* mRNA expression (284 bp) in HPDE (H) and PancTu-1 Luc (P) cells ($n = 3$). (*b*) Western blot on the whole cell lysates with polyclonal C-terminal antibody for P2X7R shows the A isoform (70 kDa). β actin (42 kDa) was used as loading control ($n = 4$). Bar graph shows the level of P2X7R protein as a ratio to β actin. Significant difference in comparison to HPDE cells $p < 0.001$ (**) is reported. (*c*) Effect of ATP and ATP plus AZ10606120 on PancTu-1 Luc cell proliferation was assayed using BrdU incorporation. Black bars show the effect of increasing concentration of exogenous ATP (0 μM, 10 μM, 100 μM and 1 mM). White bars represent the effect of increasing ATP concentration in combination with 10 μM AZ10606120 (P2X7R allosteric inhibitor). (*d*) Effect of increasing concentrations of BzATP (P2X7R agonist) on BrdU incorporation. Each run was performed in triplicates and the graphs show data from four independent experiments (mean ± SEM). Significant differences $p < 0.05$ (*, #) and $p < 0.001$ (**, ##) from the respective control, without exogenous ATP or BzATP (*, **) and with/without inhibitor (#, ##) are indicated. (*e*) The graph shows PancTu-1 Luc cell proliferation after transfection with siRNA against P2X7 mRNA (siP2X7), scramble siRNA (siSCR) and siP2X7 plus BzATP (100 μM). Data are represented as mean ± SEM. Significant differences $p < 0.001$ (**) from the control are indicated. (*f*) Western blot shows the protein expression of P2X7R in PancTu-1 Luc cells transfected with siRNA against P2X7R (siP2X7) or scramble Naito-1 siRNA as control (siSCR).

mPSCs stimulate PancTu-1 Luc cell migration—role of P2X7R

To evaluate the role of P2X7R in PancTu-1 Luc cell migration (Figs. 3*a*–3*c*), we performed a wound assay using removable inserts to minimize cell damage and ATP release. Cells were incubated either with AZ10606120, BzATP or both. PancTu-1 Luc cells closed almost 65% of the wound/gap after 30 hr. BzATP increased cell migration (Fig. 3*b*) and the wound/gap was near closure within 30 hr (Fig. 3*c*). In contrast, AZ10606120 drastically reduced cell migration and abolished BzATP effect; at the end point almost 70–80% of the wound

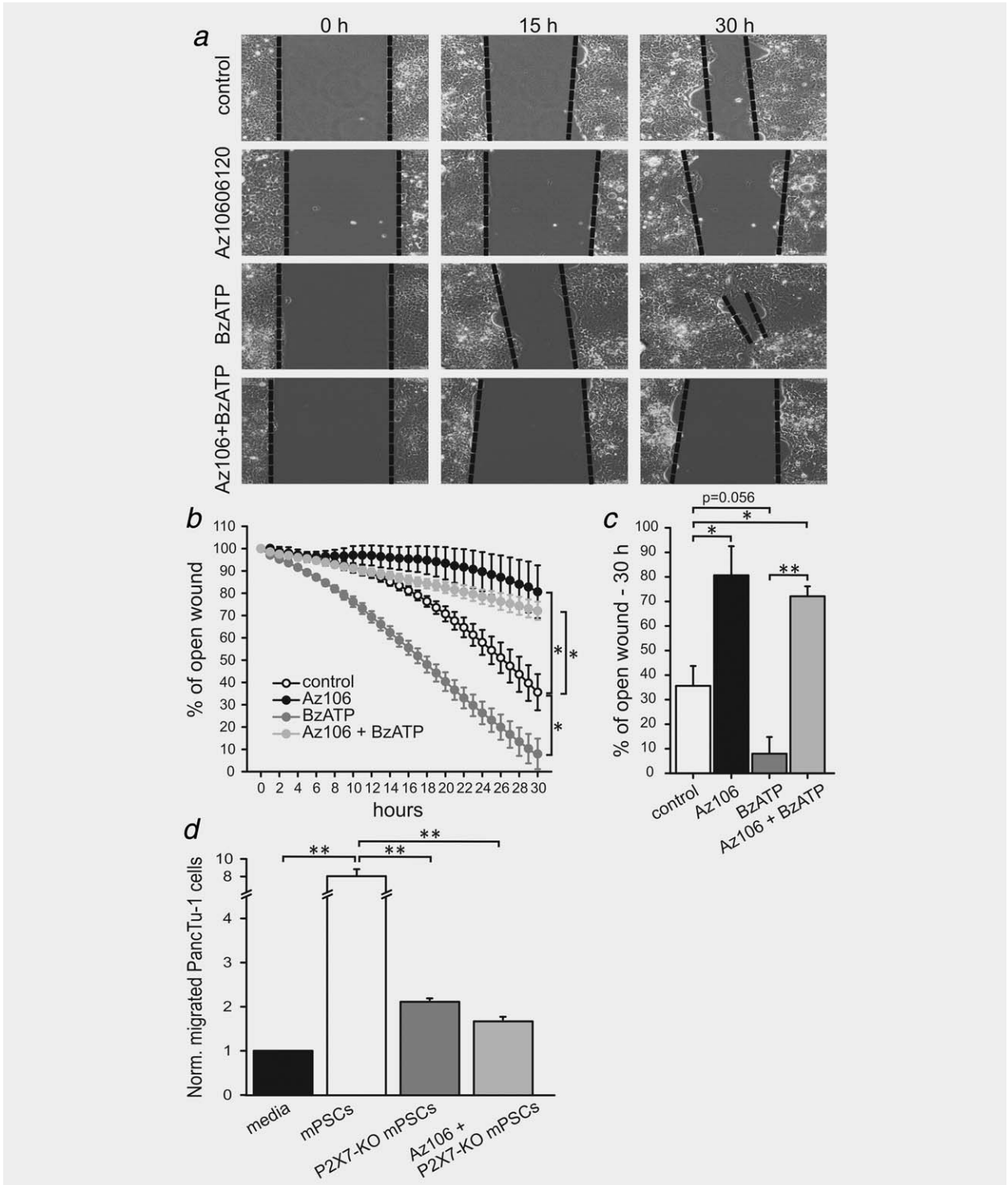

Figure 3. Effect of AZ10606120, BzATP and mPSCs on PancTu-1 Luc cells migration. PancTu-1 Luc cells were grown to confluence in the two-chamber silicon insert. After removal, phase-contrast images were taken every hour for 30 hr. (*a*) Representative images at 0, 15 and 30 hr for control, AZ10606120, BzATP and P2X7R inhibitor plus BzATP. (*b*) White, black, grey and light grey circles show the percentage of the wound/gap open every hour in control cells (vehicle); cells treated with 10 μM AZ10606120, with 10 μM BzATP and AZ10606120 plus BzATP, respectively. Significant differences $p < 0.05$ (*) between control and inhibitor/agonist was calculated from the slope of the curves after 11 hr. (*c*) The graph shows the endpoint, *i.e.,* percentage of wound still open after 30 hr; significant differences $p < 0.05$ (*) and $p \leq 0.001$ (**) are indicated. Four to seven fields of view were analyzed per each experiment. The graphs show data from 3 to 4 independent experiments (mean ± SEM). (*d*) The graph shows effect of mPSCs from wild-type and P2X7 knockout (+/−AZ10606120) on PancTu-1 Luc cells migration. The graph shows data from four independent experiments (mean ± SEM). Significant differences $p < 0.001$ (**) are indicated.

was still open (Fig. 3*c*). These results suggest that P2X7R is tonically active and involved in basal cell migration.

To determine if P2X7R plays any role in PSCs-cancer cells crosstalk, we performed Boyden chamber experiment, in which PancTu-1 Luc cells were co-cultured (upper chamber) with freshly isolated mPSCs (lower chamber) (Fig. 3*d*). We observed a remarkable increase in PancTu-1 Luc cell migration when they were stimulated by mPSCs expressing wild type P2X7R. However, when we used mPSCs isolated from $P2X7^{-/-}$ mice in the lower chamber, cancer cell migration was significantly reduced, and AZ10606120 had no further effects. This indicates that PSCs release chemotactic factors which attract cancer cells and that P2X7R plays a role in their secretion.

PancTu-1 Luc orthotopic mouse tumour model—characterization and P2X7R expression

The next objective was to confirm our *in vitro* findings on an *in vivo* cancer model. A PancTu-1 orthotopic xenograft model has been chosen for the study, similar as the one already established and characterized by Alves *et al.*,[28] as it reflects invasion and all the steps of the metastatic cascade of human PDAC. Since one of the disadvantages of an orthotopic PDAC model is the difficulty of following tumour growth and spread, the implanted luciferase-expressing PancTu-1 Luc cells allowed noninvasive bioluminescence imaging (BLI). PancTu-1 Luc cells were implanted in the head of the pancreas of athymic nude mice (Fig. 1*a*) and an extensive local tumour growth ($n = 4$, tumour take = 100%) already within 4 weeks after implantation was observed. In fixed tissue, tumour cells were visualized by staining for epidermal growth factor receptor (EGFR), a receptor that is over-expressed in PDAC.[31] PancTu-1 Luc cells formed poorly differentiated, highly EGFR-expressing tumours (Supporting Information Fig. 1a). The PancTu-1 Luc showed very aggressive tumour growth, frequently invading into the surrounding organs, such as duodenum and stomach (Supporting Information Fig. 1b) as well as the mesentery, spleen, kidney and liver (Supporting Information Figs. 1c–1f).

To validate the expression level of P2X7R in PancTu-1 Luc primary tumours and in surrounding pancreas, tissues were stained with P2X7R-targetting antibody. Additionally, consecutive sections were stained with antibody-targeting human EGFR, and with antibody targeting α-SMA expressed in mPSCs (Fig. 4*a*). The images show that between cancer cells there are dense areas populated by mPSCs. mPSCs and luminal membranes of pancreatic ducts express P2X7R. Next we stained the tumour and pancreatic sections with three different antibodies against P2X7R, which have different specificities for murine and human tissue, and potentially recognize different receptor isoforms (Figs. 4*b*–4*d*). With the two murine antibodies, directed against extracellular domain (all P2X7 splice isoforms; Fig. 4*b*) and C-terminal (nontruncated isoforms; Fig. 4*c*), the P2X7R was found in the PanIN structures, and in acinar-like structures with increased lumen size and/or small ducts, which would indicate acinar-to-ductal metaplasia. Furthermore, mPSCs stained heavily with both antibodies. The P2X7R expression in PancTu-1 Luc tumour cells was verified with the anti-P2X7R human antibody (PA5-28020-C-term) optimized for paraffin section and images show heavy expression in the tumour cells (Fig. 4*d*). The tumour-free pancreas (Fig. 4*e*) shows that P2X7R is expressed in pancreatic ducts, mPSCs and islets of Langerhans, but not in pancreatic acini, which agrees with earlier studies.[25,32,33] Similar staining was obtained in normal pancreas using immunofluorescence (data not shown).

Effect of P2X7R inhibitor AZ10606120 on tumour growth

Having established that P2X7R is expressed in the tumour niche, the next objective was to determine whether the receptor inhibitor AZ10606120 would influence the growth and spread of pancreatic cancer. Therapy regime, shown in Figure 1*b*, was started at Day 10 after cells implantation. The tumour progression was assessed by BLI. The bioluminescence was acquired before the start of the therapy as well as at Day 17, 23 and 30 postimplantation. In all mice, BLI over primary tumour area increased over time, but the treated mice revealed a reduced increment of the signal intensity compared to the nontreated group, as shown on the representative images in Figure 5*a*. The animals showed widely different BLI at day 10. In order to quantify these results, the total flux (photons/sec) over primary tumour area was measured using 2D ROIs, normalized to the total flux at Day 10 for each mouse and log-transformed. As shown in the Figure 5*b*, the control NaCl-treated group showed steeper progression in BLI with time, compared to the group treated with P2X7R allosteric inhibitor, AZ10606120. This suggests faster tumour growth, and/or higher metabolic activity of the tumour cells in the nontreated animals. AZ10606120 inhibitor had no effect on luciferin/luciferase assay *in vitro* (data not shown).

At Day 30 after the implantation mice were sacrificed. *Ex vivo* bioluminescence imaging of animals with opened abdominal cavity and explanted primary tumours confirmed the detection of luminescence signals over primary tumour mass (Supporting Information Figs. 2a and 2b). The tumour sizes were also measured *ex vivo* with caliper. Here no significant differences in the average tumour volume between treated and untreated group were detected (Supporting Information Fig. 3a); but the tumours of untreated mice showed clearly higher deviation. The difference in the results between *in vivo* BLI (significantly lower luminescence intensity in the treated group) and the tumour volume measurement during the section (no significant difference between the groups) can be explained with the fact that apparently, most of the mice randomly chosen for treatment had bigger tumour mass at the beginning of the therapy at the Day 10 than the mice chosen as controls (Supporting Information Fig. 3b). The normalization of the imaging data for BLI at beginning of the therapy corresponds to the actual progression of the primary tumour and implicates the reduction in the tumour size with the inhibitor.

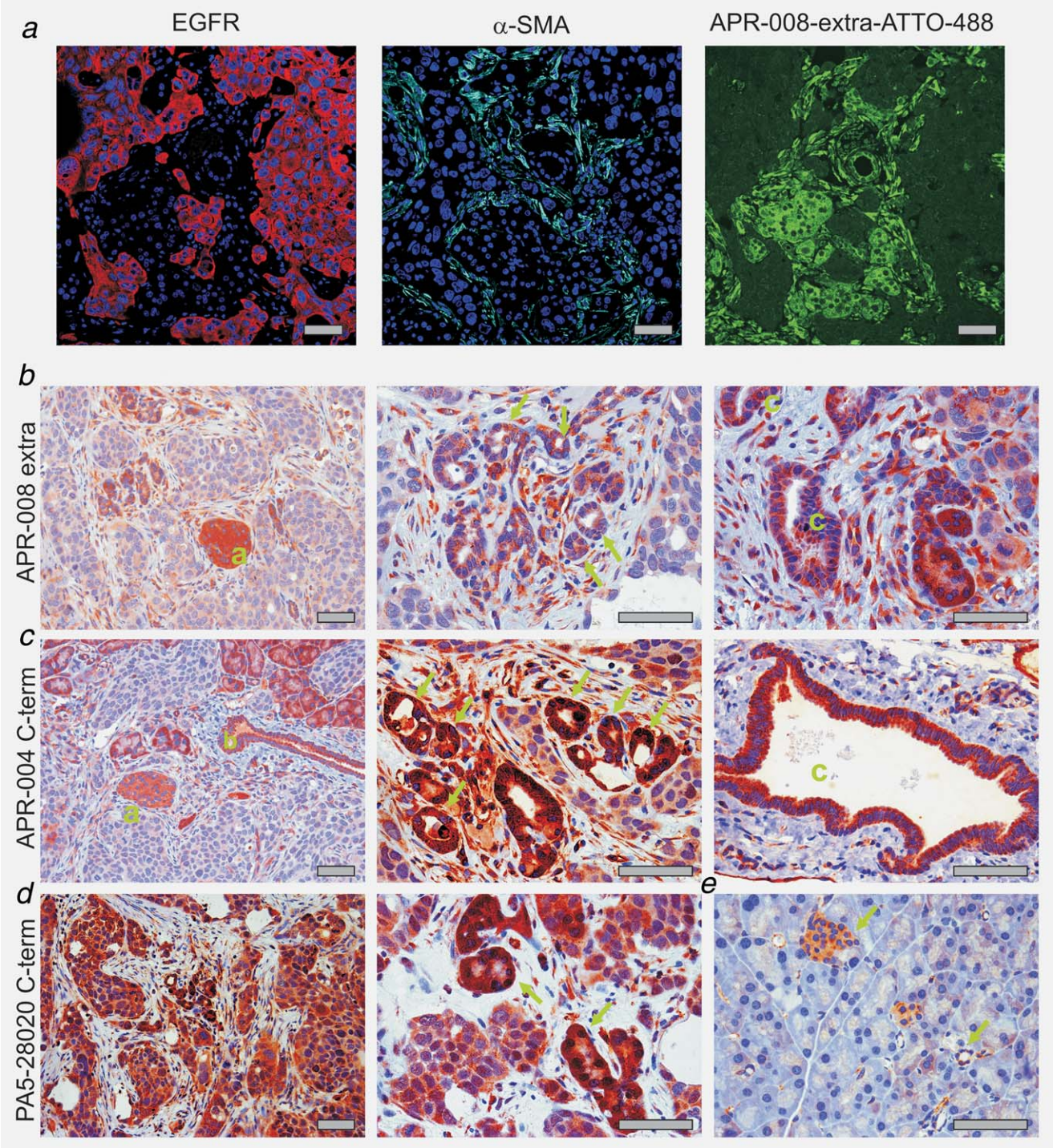

Figure 4. P2X7R expression in PancTu-1 Luc *in vivo* model. (*a*) Immunofluorescence detection of EGFR in the tumour cells (red), α-SMA for the pancreatic stellate cells (cyan) and P2X7R (ATTO-488, green). The staining was performed in two subsequent 2 μm sections. (*b–d*) Representative pictures of P2X7R expression in PancTu-1 Luc tumour paraffin sections. The slides were stained with three different P2X7R antibodies: (*b*) APR-008 against an epitope in the extracellular loop. (*c*) APR-004 against the C-terminal; (*d*) PA5-28020 against the C-terminal and more specific for human tissues embedded in paraffin. (*e*) Control of P2X7R antibody (PA5-28020) in a tumour-free pancreas of the PDAC mice. In images (*b–d*) following structures are indicated: Islets of Langerhans (a), ducts (b), PanINs (c) and acinar-like structures with increased lumen size (arrows). All images are representative of staining carried out on $n = 3–6$. Images were taken with different magnifications but scale bars are 50 μm on all panels. [Color figure can be viewed in the online issue, which is available at wileyonlinelibrary.com.]

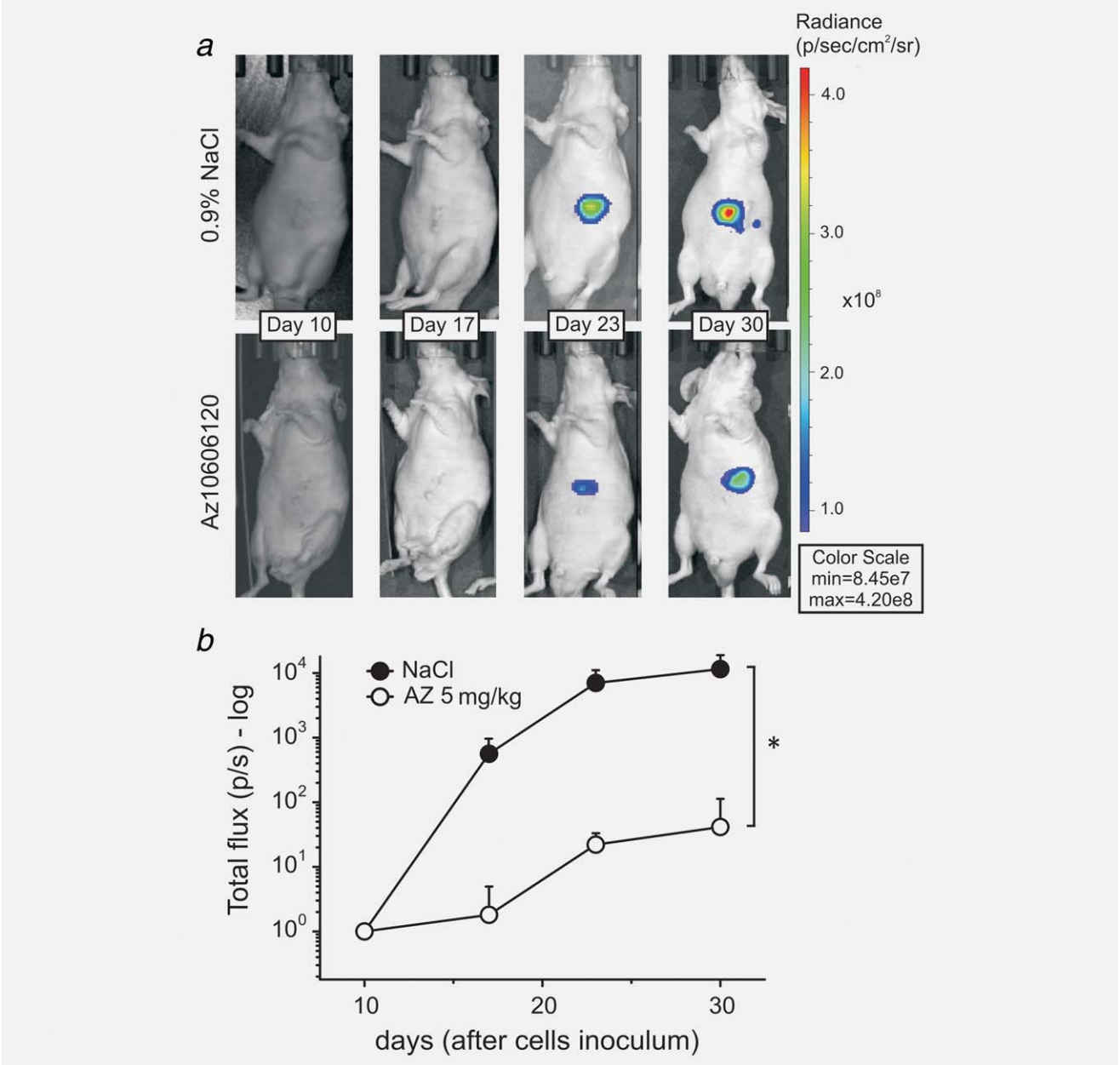

Figure 5. Effect of AZ10606120 on tumour growth.(*a*) *In vivo* representative bioluminescence images obtained by IVIS Spectrum of PancTu-1 Luc mice treated either with 0.9% NaCl (upper panel, $n = 6$) or with AZ10606120 (lower panel, $n = 7$) at day 10, 17, 23 and 30 after cells implantation. Bioluminescence signals detected 15 min after the i.p. injection of luciferin over tumour areas of the nontreated mice increased faster than in the treated group. The given images and a scale is depicting radiance at day 30 to avoid oversaturation. (*b*) The graph shows the radiances (photons/second) measured over primary tumours using 2D ROIs at the indicated days after cells implantation normalized to the total flux at day 10 for each mouse (mean ± SD). The black symbols represent the tumour growth of the mice treated with NaCl ($n = 4$) and the white symbols the tumour growth of the mice treated with AZ10606120 ($n = 4$). Progression of BLI over time indicated significant difference between NaCl and inhibitor-treated mice ($p < 0.05$ (*) slope analysis), and point to point comparison between groups is significant at day 23 and 30 ($p < 0.05$). [Color figure can be viewed in the online issue, which is available at wileyonlinelibrary.com.]

Incidence of metastases was determined during the section macroscopically and by bioluminescence imaging of further extracted organs such as mesentery, spleen, liver and kidney (Supporting Information Fig. 2c). Both treated and untreated groups showed a frequent and comparable disseminated pattern with visible metastases in those organs. Data given in the Supporting Information Figure 2d show that there was no clear difference between the two groups, indicating that P2X7R allosteric inhibitor alone is not efficient in blocking the metastatic and invasive behavior of PancTu-1 Luc cells *in vivo*.

Tumour infiltration in the surrounding organs such as stomach and duodenum was determined by EGFR staining

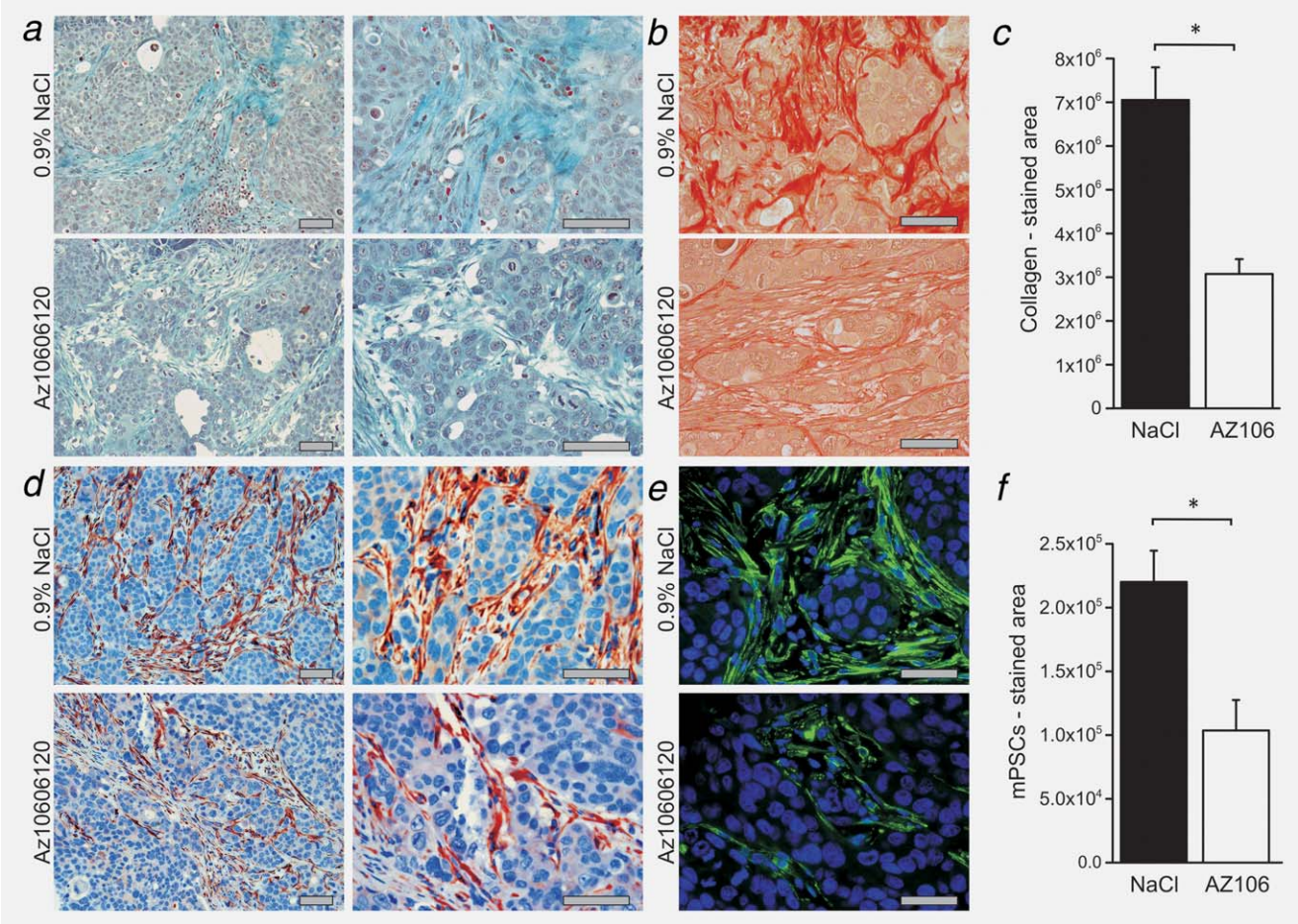

Figure 6. Effect of AZ10606120 on mPSCs and collagen deposition.Representative pictures of Masson Goldner Trichrom (*a*) and Picrosirius Red (*b*) staining of treated and untreated PancTu-1 Luc tumours. (*c*) The graph shows the difference in collagen deposition (stained area) between the NaCl and AZ10606120 groups. The staining was performed in all tumours ($n = 6–7$) and eight to nine fields of view were analyzed in each slide (see Methods). Significant difference $p < 0.05$ (*) is indicated. (*d*) Representative pictures of AEC reaction and immunofluorescence (*e*) for pancreatic stellate cells detection, using an antibody against α-SMA. (*f*) The graph shows the results of the stained area analysis of the α-SMA immunofluorescence staining in treated and untreated groups (mean ± SEM). Eight to nine fields of view, per each tumour section, were analyzed. Significant difference $p < 0.05$ (*) between NaCl and AZ10606120 mice is indicated. Different magnifications were used on right and left images in panels A and D but scale bars are all 50 μm, also in panels B and E. [Color figure can be viewed in the online issue, which is available at wileyonlinelibrary.com.]

of tumour sections (Supporting Information Fig. 4). No differences were observed between the two groups.

P2X7R inhibition reduces fibrosis and mPSC number

In order to evaluate whether there was any effect of the P2X7R inhibition on the fibrotic area and on mPSCs, immunohistochemistry and immunofluorescence studies were performed on the tumour slices. Analysis of the tumour fibrosis, using Masson Goldner trichrome staining for connective tissue (Fig. 6*a*) revealed a denser fibrosis in untreated mice compared to treated ones. Additional analysis of the fibrosis composition using Picrosirius Red staining for collagen I and III (Figs. 6*b*–6*c*), showed that the treatment with P2X7R allosteric inhibitor caused a reduction in collagen production/deposition, visible also in a more loose structure of collagen fibres and lower intensity staining (Fig. 6*b*). This was further quantified as stained areas using Image J (Fig. 6*c*) and data show that AZ10606120 clearly and significantly reduced the tumour fibrosis.

It is well known that PSCs are the principal source of collagen in the stroma in response to pancreatic injury.[34] Moreover, in a previous study, our group showed that the P2X7R allosteric inhibitor AZ10606120 considerably reduced *in vitro* mPSCs proliferation.[25] Therefore, to understand if the reduction in collagen deposition was related to the reduced number and/or activity of mPSCs, we stained the tumour sections with α-SMA antibody. Immunohistochemical images (Fig. 6*d*) show denser α-SMA in tumours of control animals. In order to quantify mPSCs staining, we used immunofluorescence imaging (Fig. 6*e*) and quantified the area occupied by mPSCs. The data presented in Figure 6*f* clearly show that treatment of the mice with AZ10606120

resulted in the reduction of the area covered by mPSCs, indicating possibly lower number or less active cells.

Discussion

In this study we showed that P2X7R regulates proliferation of PancTu-1 Luc cancer cells *in vitro* and promotes the migration of PancTu-1 Luc under mPSCs stimuli. We also demonstrated that these functions could be inhibited by the P2X7R inhibitor AZ10606120 *in vitro*. Based on these findings, we evaluated the efficacy of AZ10606120 on PancTu-1 Luc orthotopic pancreatic tumour-bearing mice using *in vivo* bioluminescence imaging to monitor PDAC growth and spread. We demonstrated that P2X7R is expressed in primary tumour cells and in mPSCs and that AZ10606120 decreases tumour bioluminescence as well as mPSCs cell activity/number and collagen deposition. However, treatment of mice with the inhibitor had no effect on tumour invasion and spread to the other organs.

The P2X7 receptor is expressed in PancTu-1 Luc at the mRNA and protein levels (Figs. 2*a* and *b*), and the protein expression is higher in the tumour cells compared to HPDE cells. This finding agrees with our previous study on the receptor expression in other PDAC cell lines,[24] and with several studies performed on different cancer types, *e.g.,* breast cancer, nonsmall cell lung cancer[35] and melanoma.[36] In our study, stimulation of PancTu-1 Luc with increasing exogenous concentrations of ATP or BzATP decreased cell proliferation/survival, similar to other PDAC cell lines and reports on other cancer cells.[24,29,37] The allosteric inhibitor of P2X7R, AZ10606120, significantly reduced BrdU incorporation, due to an arrest of cell proliferation. The inhibitor was effective even without exogenous ATP, and presuming that the inhibitor is specific, it implicates that the receptor was tonically/basally active in our PDAC cell model. These conclusions were supported by experiments with siRNA. Similar effect of P2X7R on cell survival and effects of the allosteric inhibition of P2X7R were also shown on mouse pancreatic stellate cells,[25] ovarian carcinoma cells[38] and *in vivo* on melanoma cancer model.[20]

An important characteristic that makes PDAC aggressive is the ability of tumour cells to migrate and invade the surrounding or distant tissues. Here, we demonstrated that cancer cells migration was increased *in vitro* by P2X7R stimulation and inhibited by AZ10606120 (Figs 3*a*–3*c*). Our data are in line with other studies showing the role of P2X7R in migration in breast cancer cells,[18,39] lung cancer cells[40] and prostate cancer cells.[41] In stroma-rich PDAC interplay between cancer cells and PSCs, which has been termed as the "deadly symbiosis", leads to a massive cancer cell migration and invasion.[42] Here, we showed that P2X7R is important in enhancing cancer cell migration and/or chemotactic factor release suggesting interaction between PDACs and PSCs (Fig. 3*d*).

In vivo, the implanted PancTu-1 Luc primary tumours clearly expressed P2X7R (Fig. 4). The luciferase activity allowed us to follow the tumour growth by detecting the bioluminescent signal after i.p. luciferin injection. It appears that the group of tumour-bearing mice treated with AZ10606120 showed a lower increase in bioluminescence over time compared to mice that received the vehicle. This validates that the P2X7R allosteric inhibitor AZ10606120 has anti-proliferative effects both *in vitro* and *in vivo*. This inhibitor is not yet widely tested in cancer, but two studies show that similar anti-proliferative effect of the inhibitor was detected in subcutaneous cancer induced by HEK293-hP2X7 or B16 melanoma cells.[1,20]

We found P2X7R expressed in pancreatic ducts and PSCs, and islets of Langerhans, as expected from other expression and functional studies of normal pancreas.[25,32,33,43] There was a significant increase in PanIN structures that were heavily stained with P2X7R antibody in tumour vicinity. Interestingly, acinar-like structures with increased lumen size, in/close to the tumour mass, showed heavy expression of P2X7R. Notably, normal rodent acini do not express P2X7R on the protein level (Fig. 4) or on mRNA level or functional level.[44] This implies that implantation of human cancer cells induces P2X7R overexpression in murine pancreatic tissue of epithelial origin: ductal neoplasia and acinar-to-duct metaplasia.

Pancreatic stellate cells play an important role in this desmoplastic reaction by synthetizing a large amount of extracellular matrix proteins, such as collagens.[8] Here we show that administration of P2X7R inhibitor reduced the number or activity of mPSCs and this correlated with a reduction of collagen deposition (Figs. 6*b*–6*f*) resulting in a less rigid stromal reaction. These findings correlated also with the high expression of P2X7R in mPSCs showed in Figures 4*a*–4*d* and with the *in vitro* anti-proliferative effect of AZ10606120 on mPSCs showed in our previous study.[25] Nevertheless, at this stage more basic knowledge regarding targeting of PSCs and desmoplasia is needed. Recent publication in PDAC research question whether inhibition of stroma and fibrosis is advantageous as, on one hand, it may improve the drug delivery but, on the other hand, it may remove restrain on tumour growth and metastasis.[45–47]

The P2X7 receptor is a therapeutic target not only in cancer but in several diseases, such as rheumatoid arthritis, Alzheimer's disease, respiratory diseases and renal diseases,[48,49] and several P2X7R inhibitors are currently in phase I and II of clinical trials.[48] AZ10606120 was not yet so widely used, except in a couple of subcutaneous cancer models.[1,20] Our application to the PDAC orthotopic model indicates relatively high efficacy (i.p. 5 mg/kg) in inhibiting both mPSCs as well as PDAC cells compared to other P2X7R inhibitors.[50]

In vivo we could not show any significant effects of the inhibitor on invasion and metastasis development, although *in vitro* we have seen clear effects of the inhibitor on PancTu-1 Luc cell migration. It is possible that, despite of the high P2X7R over-expression of PancTu-1 Luc cells, the invasion and metastatic behavior of the undifferentiated tumours formed by these cells *in vivo* is too aggressive to be

blocked only by this inhibitor alone. In this context, a less aggressive and more differentiated P2X7R over-expressing PDAC mouse model could be more useful, such as Capan-1 or Capan-2 xenografts, which become clinically symptomatic in about 90 days after cell injection,[31] as compared to 30 days needed by the PancTu-1 Luc cells. Furthermore, we might need to consider polymorphisms of the P2X7 receptor and heterogeneity of cancer cells. For example, tumours might contain both pro-apoptotic/necrotic P2X7R isoforms (or SNPs) as well as trophic receptor variants that support growth and metastasis. Lastly, as discussed above, consequences of targeting of tumour-stroma may have complex outcomes.

Conclusion

In conclusion, our work shows that P2X7R plays an important role in several aspects of *in vivo* and *in vitro* PDAC progression. Therefore, P2X7R inhibition might decrease pancreatic cancer aggressiveness, acting on multiple fronts—PDAC proliferation, interaction of cancer cells and PSCs, PSCs viability and collagen deposition. The AZ10606120 anti-proliferative effect on cancer cells and the reduction of pancreatic cancer-associated fibrosis could open a new possibility for pancreatic cancer treatment co-targeting cells in the pancreatic tumour microenvironment. In order to proceed in this direction more refined P2X7R models, including immune systems, are needed as well more thorough understanding of the role of this receptor in stroma-tumour interaction and metastasis.

Acknowledgement

We are grateful to Prof. Dr. Holger Kalthoff from University Hospital Schleswig-Holstein in Kiel, for providing PancTu-1 Luc cell line and Dr. M.S. Tsao, University Health Network in Toronto, for the gift of HPDE cells and Prof. Niklas R. Jørgensen, Department of Clinical Biochemistry, Rigshospitalet, Glostrup for gift of P2X7R$^{-/-}$ mice. Special thanks to Pernille Roshof, Bärbel Heidrich and Roswitha Streich for the technical assistance. Images were taken at the Center for Advanced Bioimaging, University of Copenhagen.

References

1. Adinolfi E, Capece M, Franceschini A, et al. Accelerated tumor progression in mice lacking the ATP receptor P2X7. *Cancer Res* 2015; 75: 635–44.
2. Partensky C. Toward a better understanding of pancreatic ductal adenocarcinoma: glimmers of hope? *Pancreas* 2013; 42:729–39.
3. Kramer-Marek G, Gore J, Korc M. Molecular imaging in pancreatic cancer—a roadmap for therapeutic decisions. *Cancer Lett* 2013; 341:132–8.
4. Garrido-Laguna I, Hidalgo M. Pancreatic cancer: from state-of-the-art treatments to promising novel therapies. *Nat Rev Clin Oncol* 2015; 12: 319–34.
5. Rhim AD, Mirek ET, Aiello NM, et al. EMT and dissemination precede pancreatic tumor formation. *Cell* 2012; 148:349–61.
6. Aichler M, Seiler C, Tost M, et al. Origin of pancreatic ductal adenocarcinoma from atypical flat lesions: a comparative study in transgenic mice and human tissues. *J Pathol* 2012; 226:723–34.
7. Gidekel Friedlander SY, Chu GC, Snyder EL, et al. Context-dependent transformation of adult pancreatic cells by oncogenic K-Ras. *Cancer Cell* 2009; 16:379–89.
8. Tang D, Wang D, Yuan Z, et al. Persistent activation of pancreatic stellate cells creates a microenvironment favorable for the malignant behavior of pancreatic ductal adenocarcinoma. *Int J Cancer* 2013; 132:993–1003.
9. Pellegatti P, Raffaghello L, Bianchi G, et al. Increased level of extracellular ATP at tumor sites: in vivo imaging with plasma membrane luciferase. *PLoS One* 2008; 3:e2599
10. Roger S, Pelegrin P. P2X7 receptor antagonism in the treatment of cancers. *Expert Opin Investig Drugs* 2011; 20:875–80.
11. Jiang LH, Baldwin JM, Roger S, et al. Insights into the molecular mechanisms underlying mammalian P2X7 receptor functions and contributions in diseases, revealed by structural modeling and single nucleotide polymorphisms. *Front Pharmacol* 2013; 4:55
12. Sluyter R, Stokes L. Significance of P2X7 receptor variants to human health and disease. *Recent Pat DNA Gene Seq* 2011; 5:41–54.
13. Surprenant A, Rassendren F, Kawashima E, et al. The cytolytic P2Z receptor for extracellular ATP identified as a P2X receptor (P2X7). *Science* 1996; 272:735–8.
14. Virginio C, MacKenzie A, North RA, et al. Kinetics of cell lysis, dye uptake and permeability changes in cells expressing the rat P2X7 receptor. *J Physiol* 1999; 519:335–46.
15. Baroja-Mazo A, Barbera-Cremades M, Pelegrin P. The participation of plasma membrane hemichannels to purinergic signaling. *Biochim Biophys Acta* 2013; 1828:79–93.
16. Greig AV, Linge C, Healy V, et al. Expression of purinergic receptors in non-melanoma skin cancers and their functional roles in A431 cells. *J Invest Dermatol* 2003; 121:315–27.
17. White N, Knight GE, Butler PE, et al. An in vivo model of melanoma: treatment with ATP. *Purinergic Signal* 2009; 5:327–33.
18. Jelassi B, Chantome A, Alcaraz-Perez F, et al. P2X(7) receptor activation enhances SK3 channels- and cystein cathepsin-dependent cancer cells invasiveness. *Oncogene* 2011; 30:2108–22.
19. Solini A, Cuccato S, Ferrari D, et al. Increased P2X7 receptor expression and function in thyroid papillary cancer: a new potential marker of the disease? *Endocrinology* 2008; 149:389–96.
20. Adinolfi E, Raffaghello L, Giuliani AL, et al. Expression of P2X7 receptor increases in vivo tumor growth. *Cancer Res* 2012; 72:2957–69.
21. Adinolfi E, Cirillo M, Woltersdorf R, et al. Trophic activity of a naturally occurring truncated isoform of the P2X7 receptor. *Faseb J* 2010; 24: 3393–404.
22. Wilhelm K, Ganesan J, Muller T, et al. Graft-versus-host disease is enhanced by extracellular ATP activating P2X7R. *Nat Med* 2010; 16:1434–8.
23. Ravenna L, Sale P, Di Vito M, et al. Up-regulation of the inflammatory-reparative phenotype in human prostate carcinoma. *Prostate* 2009; 69: 1245–55.
24. Giannuzzo A, Pedersen SF, Novak I. The P2X7 receptor regulates cell survival, migration and invasion of pancreatic ductal adenocarcinoma cells. *Mol Cancer* 2015; 14:203
25. Haanes KA, Schwab A, Novak I. The P2X7 receptor supports both life and death in fibrogenic pancreatic stellate cells. *PLoS One* 2012; 7:e51164
26. Ouyang H, Mou L, Luk C, et al. Immortal human pancreatic duct epithelial cell lines with near normal genotype and phenotype. *Am J Pathol* 2000; 157:1623–31.
27. Syberg S, Petersen S, Beck Jensen JE, et al. Genetic background strongly influences the bone phenotype of P2X7 receptor knockout mice. *J Osteoporos* 2012; 2012:391097
28. Alves F, Contag S, Missbach M, et al. An orthotopic model of ductal adenocarcinoma of the pancreas in severe combined immunodeficient mice representing all steps of the metastatic cascade. *Pancreas* 2001; 23:227–35.
29. Brandao-Burch A, Key ML, Patel JJ, et al. The P2X7 receptor is an important regulator of extracellular ATP levels. *Front Endocrinol (Lausanne)* 2012; 3:41
30. Smith SM, Mitchell GS, Friedle SA, et al. Hypoxia attenuates purinergic P2X receptor-induced inflammatory gene expression in brainstem microglia. *Hypoxia (Auckl)* 2013; 1:1–11.
31. Cardone RA, Greco MR, Zeeberg K, et al. A novel NHE1-centered signaling cassette drives epidermal growth factor receptor-dependent pancreatic tumor metastasis and is a target for combination therapy. *Neoplasia* 2015; 17:155–66.
32. Novak I, Jans IM, Wohlfahrt L. Effect of P2X(7) receptor knockout on exocrine secretion of pancreas, salivary glands and lacrimal glands. *J Physiol* 2010; 588:3615–27.
33. Coutinho-Silva R, Robson T, Beales PE, et al. Changes in expression of P2X7 receptors in NOD mouse pancreas during the development of diabetes. *Autoimmunity* 2007; 40:108–16.
34. McCarroll JA, Naim S, Sharbeen G, et al. Role of pancreatic stellate cells in chemoresistance in pancreatic cancer. *Front Physiol* 2014; 5:141

35. Jelassi B, Anchelin M, Chamouton J, et al. Anthraquinone emodin inhibits human cancer cell invasiveness by antagonizing P2X7 receptors. *Carcinogenesis* 2013; 34:1487–96.
36. Hattori F, Ohshima Y, Seki S, et al. Feasibility study of B16 melanoma therapy using oxidized ATP to target purinergic receptor P2X7. *Eur J Pharmacol* 2012; 695:20–6.
37. Jun DJ, Kim J, Jung SY, et al. Extracellular ATP mediates necrotic cell swelling in SN4741 dopaminergic neurons through P2X7 receptors. *J Biol Chem* 2007; 282:37350–8.
38. Vazquez-Cuevas FG, Martinez-Ramirez AS, Robles-Martinez L, et al. Paracrine stimulation of P2X7 receptor by ATP activates a proliferative pathway in ovarian carcinoma cells. *J Cell Biochem* 2014; 115:1955–66.
39. Xia J, Yu X, Tang L, et al. P2X7 receptor stimulates breast cancer cell invasion and migration via the AKT pathway. *Oncol Rep* 2015;103–10.
40. Takai E, Tsukimoto M, Harada H, et al. Autocrine signaling via release of ATP and activation of P2X7 receptor influences motile activity of human lung cancer cells. *Purinergic Signal* 2014; 10:487–97.
41. Qiu Y, Li WH, Zhang HQ, et al. P2X7 mediates ATP-driven invasiveness in prostate cancer cells. *PLoS One* 2014; 9:e114371
42. Vonlaufen A, Joshi S, Qu C, et al. Pancreatic stellate cells: partners in crime with pancreatic cancer cells. *Cancer Res* 2008; 68:2085–93.
43. Kunzli BM, Nuhn P, Enjyoji K, et al. Disordered pancreatic inflammatory responses and inhibition of fibrosis in CD39-null mice. *Gastroenterology* 2008; 134:292–305.
44. Novak I, Nitschke R, Amstrup J. Purinergic receptors have different effects in rat exocrine pancreas. Calcium signals monitored by fura-2 using confocal microscopy. *Cell Physiol Biochem* 2002; 12:83–92.
45. Rhim AD, Oberstein PE, Thomas DH, et al. Stromal elements act to restrain, rather than support, pancreatic ductal adenocarcinoma. *Cancer Cell* 2014; 25:735–47.
46. Ozdemir BC, Pentcheva-Hoang T, Carstens JL, et al. Depletion of carcinoma-associated fibroblasts and fibrosis induces immunosuppression and accelerates pancreas cancer with reduced survival. *Cancer Cell* 2014; 25:719–34.
47. Provenzano PP, Cuevas C, Chang AE, et al. Enzymatic targeting of the stroma ablates physical barriers to treatment of pancreatic ductal adenocarcinoma. *Cancer Cell* 2012; 21: 418–29.
48. Arulkumaran N, Unwin RJ, Tam FW. A potential therapeutic role for P2X7 receptor (P2X7R) antagonists in the treatment of inflammatory diseases. *Expert Opin Investig Drugs* 2011; 20: 897–915.
49. Bartlett R, Stokes L, Sluyter R. The P2X7 receptor channel: recent developments and the use of P2X7 antagonists in models of disease. *Pharmacol Rev* 2014; 66:638–75.
50. Hansen RR, Nielsen CK, Nasser A, et al. P2X7 receptor-deficient mice are susceptible to bone cancer pain. *Pain* 2011; 152:1766–76.